HHS Public Access

Author manuscript

Bioorg Med Chem. Author manuscript; available in PMC 2016 March 01.

Published in final edited form as:

Bioorg Med Chem. 2015 March 1; 23(5): 1169–1178. doi:10.1016/j.bmc.2014.12.035.

Synthesis and Comparative Biological Evalution of Bifunctional Ligands for Radiotherapy Applications of ^{90}Y and ^{177}Lu

Hyun-Soon Chong[1,*], **Xiang Sun**[1], **Yunwei Chen**[1], **Inseok Sin**[1], **Chi Soo Kang**[1], **Michael R. Lewis**[2,3], **Dijie Liu**[3], **Varyanna C. Ruthengael**[3], **Yongliang Zhong**, **Ningjie Wu**[1], and **Hyun A Song**[1]

[1]Chemistry Division, Department of Biological and Chemical Sciences, Illinois Institute of Technology, Chicago, IL

[2]Research Service, Harry S. Truman Memorial Veterans' Hospital, Columbia, MO

[3]Department of Veterinary Medicine and Surgery, University of Missouri, Columbia, MO

Abstract

Zevalin® is an antibody-drug conjugate radiolabeled with a cytotoxic radioisotope (^{90}Y) that was approved for radioimmunotherapy (RIT) of B-cell non-Hodgkin's lymphoma. A bifunctional ligand that displays favorable complexation kinetics and *in vivo* stability is required for effective RIT. New bifunctional ligands 3p-*C*-DE4TA and 3p-*C*-NE3TA for potential use in RIT were efficiently prepared by the synthetic route based on regiospecific ring opening of aziridinium ions with prealkylated triaza- or tetraaza-backboned macrocycles. The new bifunctional ligands 3p-*C*-DE4TA and 3p-*C*-NE3TA along with the known bimodal ligands 3p-*C*-NETA and 3p-*C*-DEPA were comparatively evaluated for potential use in targeted radiotherapy using β-emitting radionuclides ^{90}Y and ^{177}Lu. The bifunctional ligands were evaluated for radiolabeling kinetics with ^{90}Y and ^{177}Lu, and the corresponding ^{90}Y or ^{177}Lu-radiolabeled complexes were studied for *in vitro* stability in human serum and *in vivo* biodistribution in mice. The results of the comparative complexation kinetic and stability studies indicate that size of macrocyclic cavity, ligand denticity, and bimodality of donor groups have a substantial impact on complexation of the bifunctional ligands with the radiolanthanides. The new promising bifunctional chelates in the DE4TA and NE3TA series were rapid in binding ^{90}Y and ^{177}Lu, and the corresponding ^{90}Y- and ^{177}Lu-radiolabeled complexes remained inert in human serum or in mice. The *in vitro* and *in vivo* data show that 3p-*C*-DE4TA and 3p-*C*-NE3TA are promising bifunctional ligands for targeted radiotherapy applications of ^{90}Y and ^{177}Lu.

*To whom correspondence should be addressed. Chong@iit.edu, Phone: 312-567-3235, Fax: 312-567-3494. Mailing address: 3101 S. Dearborn St, LS 182, Department of Biological and Chemical Science, Illinois Institute of Technology, Chicago, IL, 60616.

Supporting material. ITLC chromatograms for assessment of radiolabeling reaction kinetics and serum stability and *in vivo* biodistribution data. This material is available free of charge via the Internet.

Keywords

bifunctional ligands; Y-90; Lu-177; radioimmuotherapy

1. Introduction

^{90}Y ($t_{1/2}$ = 2.7 days, E_{max} = 2.3 MeV) and ^{177}Lu ($t_{1/2}$ = 6.7 days, E_{max} = 0.5 MeV) are β-emitting cytotoxic radionuclides for use in targeted radiation therapy of cancer.[1–3] ^{90}Y is a pure β-emitter with a high energy and long range of tissue penetration (~12 mm) that may be suitable for treatment of large solid tumors.[1] A ^{90}Y-radiolabeled antibody conjugate (Zevalin®) is clinically available for radioimmunotherapy (RIT) of B-cell non-Hodgkin's lymphoma.[1,4] ^{177}Lu possesses a shorter penetration range (~2 mm) and lower maximal energy relative to ^{90}Y and was proposed to selectively target to small tumors while minimizing tissue damage.[1,2] An imageable γ-ray of a low abundance emitted from ^{177}Lu can be applied for a gamma scintigraphy during radiation therapy.[1]

An effective RIT using a radiolanthanide requires the use of a bifunctional ligand that can form a metal complex with high thermodynamic stability and rapid radiolabeling kinetics under mild conditions.[5,6] The radiolabeled complexes for RIT also must kinetically inert to transchelation by metal cations and natural chelators present *in vivo*.[5,6] Although efficacy and potency of RIT have been demonstrated in numerous clinical trials, lack of an optimal bifunctional ligands remains one of limitations for practical applications of RIT.[1–4] Research effort has been made to improve chelation chemistry for RIT applications of ^{90}Y and ^{177}Lu. Better understanding of chelation chemistry of Y(III) and Lu(III) can lead to a rational design and development of bifunctional chelators for potent and safe RIT applications using the radiolanthanides.

Y(III) and Lu(III) with the prevalent oxidation state (+3) have the respective ionic radius (pm)[7] of 116 and 98 for coordination number 8. An effective chelate of Y(III) and Lu(III) should possesses the adequate denticity to completely saturate the coordination sphere of Y(III) or Lu(III) with high complex stability. Y(III) and Lu(III) with a large ionic radius were shown to be coordinated to the chelators of high denticity such as octadentate DOTA and DTPA.[6] A size-fit between ionic radius of a metal and a macrocyclic cavity is important for an optimal complexation of a chelate with a metal.[8,9] Hexadentate NOTA was known to be ineffective in binding the lanthanides with high complex stability due to inadequate size of the macrocyclic cavity and insufficient number of donor groups in the chelator.[10–12] Octadentate DOTA, with a larger macrocyclic platform, forms stable complexes with Y(III) and Lu(III), although slow complexation kinetics of DOTA with the lanthanides remains a major drawback for its practical RIT applications.[13,14] In general, acyclic chelators such as DTPA analogues rapidly bind to a metal. However, acyclic DTPA are known to form less stable complexes than macrocyclic DOTA. The currently available RIT drug, Zevalin® was generated using a DTPA analogue (1B4M-DTPA) that displays favorable radiolabeling kinetics with ^{90}Y.[1]

Recently, we reported that bimodal ligands in the NETA and DEPA series (Figure 1), containing both macrocyclic and acyclic binding moieties, are highly effective in binding α-,

β-, or γ emitting radionuclides.[12,14–18] The design of the bimodal chelates is based on hypothesis that the chelators sequester a metal with enhanced complexation kinetics and a high level of complex stability via cooperative and bimodal coordination of macrocyclic and acyclic binding moieties. We proposed that the acyclic pendant donor groups in the chelates can rapidly capture and initiate coordination of the metal, as in the case of the acyclic chelate DTPA, and the macrocyclic component tightly wraps up the cation trapped in the acyclic donor groups achieving maximum complex stability, as in the case of a macrocyclic chelate NOTA or DOTA.[12] The octadentate NETA conjugated to trastuzumab, a tumor-targeting antibody, was found to instantly complex ^{90}Y and ^{177}Lu, and the corresponding ^{90}Y or ^{177}Lu-radiolabeled complexes were stable in human serum and tumor-bearing mice.[14]

In our continued effort in development of superior chelation chemistry for ^{90}Y and ^{177}Lu, we sought comparative evaluation of bimodal chelates for understanding on the effect of denticity, the size-match between cavity and metal, and bimodality on complexation. The new bifunctional chelates 3p-*C*-DE4TA (**1**) and 3p-*C*-NE3TA (**2**) and 3p-*C*-NOTA (**3**) were designed for evaluation of complexation with ^{90}Y and ^{177}Lu (Figure 1). The known bimodal chelates decadentate 3p-*C*-DEPA (**4**)[17] and octadentate 3p-*C*-NETA (**5**)[16] were also evaluated for complexation with ^{90}Y and ^{177}Lu for comparison. The comparative evaluation of the bimodal chelates with the structural variations is expected to advance our understanding on effect of the coordination factors including bimodality, denticity, and macrocyclic cavity on complexation of the bimodal chelates with the β-emitting radiolanthanides.

2. Materials and Methods

2.1. Instruments and reagents

^{1}H, ^{13}C, and DEPT NMR spectra were obtained using a Bruker 300 instrument and chemical shifts are reported in parts per million (ppm) on the δ scale relative to TMS. Electrospray (ESI) high-resolution mass spectra (HRMS) were obtained on JEOL double sector JMS-AX505HA mass spectrometer (University of Notre Dame, South Bend, IN). ^{90}Y (0.05M HCl) and ^{177}Lu (0.05M HCl) were purchased from Perkin Elmer.

2.1. 2-{[(2,4-dimethoxyphenyl)methyl]amino}-5-(4-nitrophenyl)pentan-1-ol (6)

To a stirred solution of **5**[16] (1.60 g, 7.13 mmol) in 1,2-dichloroethane (40 mL) was added 2,4-dimethoxy-benzaldehyde (1.19 g, 7.13 mmol). The resulting solution was stirred for 10 min, and sodium triacetoxyborohydride (2.12 g, 9.99 mmol) was added portionwise to the solution over 10 min. The mixture was stirred at room temperature for 1 d. The reaction mixture was quenched by saturated $NaHCO_3$ (100 mL), and the resulting solution was extracted with ethyl acetate (3 × 60 mL). The combined organic layer was concentrated *in vacuo*. The residue was purified by silica gel (60–230 mesh) column chromatography eluted with 10% CH_3OH in CH_2Cl_2 to afford **6** (1.65 g, 62%). ^{1}H NMR ($CDCl_3$, 300 MHz) δ 1.41–1.53 (m, 2H), 1.55–1.73 (m, 2H), 2.45 (s, 2H), 2.59–2.76 (m, 3H), 3.32 (dd, J = 10.8, 5.4 Hz, 1H), 3.61–3.74 (m, 3H), 3.78 (s, 6H), 6.34–6.49 (m, 2H), 7.07 (d, J = 7.8 Hz, 1H), 7.27 (d, J = 8.7 Hz, 2H), 8.10 (d, J = 8.7 Hz, 2H); ^{13}C NMR ($CDCl_3$, 75 MHz) δ 27.3 (t),

31.3 (t), 35.8 (t), 46.1 (t), 55.3 (q), 55.4 (q), 57.4 (d), 62.7 (t), 98.7 (d), 103.9 (d), 120.5 (s), 123.6 (d), 129.1 (d), 130.5 (d), 146.4 (s), 150.1 (s), 158.6 (s), 160.4 (s). HRMS (Positive ion ESI) Calcd for $C_{20}H_{27}N_2O_5$ $[M + H]^+$ *m/z* 375.1914. Found: $[M + H]^+$ *m/z* 375.1886.

2.2. *tert*-butyl 2-{[(2,4-dimethoxyphenyl)methyl][1-hydroxy-5-(4-nitrophenyl)pentan-2-yl]amino}acetate (7)

To a stirred solution of **6** (1.60 g, 4.27 mmol) in CH_3CN (30 mL) at 0 °C was added K_2CO_3 (0.62 g, 4.49 mmol). A solution of *t*-butyl bromoacetate (0.88 g, 4.49 mmol) in CH_3CN (10 mL) was added dropwise to the resulting mixture over 10 min. The reaction mixture was stirred for at room temperature for 2 days, while the reaction progress was continuously monitored using TLC. The reaction mixture was filtered and evaporated *in vacuo* to provide **7** (1.21 g, 91%) as a light yellow oil. The product was directly used for the next step without further purification. ^{1}H NMR ($CDCl_3$, 300 MHz) δ 1.33 (s, 9H), 1.55–1.73 (m, 4H), 2.62–2.73 (m, 2H), 2.80–2.94 (m, 1H), 3.12 (d, *J* = 17.4 Hz, 1H), 3.22 (d, *J* = 17.4 Hz, 1H), 3.33 (dd, *J* = 10.2 Hz, 10.2 Hz, 1H), 3.41–3.50 (m, 1H), 3.65 (d, *J* = 13.8 Hz, 1 H), 3.79 (s, 6 H), 4.05–4.16 (m, 1H), 6.35–6.46 (m, 2H), 7.13 (d, *J* = 8.7 Hz, 1H), 7.28 (d, *J* = 8.1 Hz, 2H), 8.10 (d, *J* = 8.1 Hz, 2H); ^{13}C NMR ($CDCl_3$, 75 MHz) δ 27.0 (t), 27.9 (q), 28.4 (t), 35.9 (t), 49.5 (t), 52.2 (t), 55.2 (q), 55.3 (q), 62.1 (t), 63.7 (d), 80.9 (s), 98.4 (d), 103.9 (d), 119.1 (s), 123.6 (d), 129.1 (d), 131.4 (d), 146.4 (s), 150.0 (s), 158.9 (s), 160.4 (s), 172.3 (s). HRMS (Positive ion ESI) Calcd for $C_{26}H_{37}N_2O_7$ $[M + H]^+$ *m/z* 489.2595. Found: $[M + H]^+$ *m/z* 489.2577.

2.3. *tert*-butyl 2-{[(2,4-dimethoxyphenyl)methyl][2-iodo-5-(4-nitrophenyl)pentyl]amino}acetate (8)

To a solution of **7** (100 mg, 0.205 mmol) and PPh_3 (64.42 mg, 0.246 mmol) in $CHCl_3$ (5 mL) at 0 °C was added portionwise I_2 (62.34 mg, 0.246 mmol) and imidazole (16.75 mg, 0.246 mmol) over 5 min. The resulting mixture was stirred for 5 h at room temperature. The solvent was evaporated, and the residue was purified by silica gel column chromatography eluted with 5% EtOAc in hexanes to afford pure **8** (97.4 mg, 86%) as a light yellow oil. Compound **8** was directly used for the next step. ^{1}H NMR ($CDCl_3$, 300 MHz) δ 1.46 (s, 9H), 1.63–1.78 (m, 2H), 1.82–2.06 (m, 2H), 2.59–2.80 (m, 2H), 2.97 (dd, *J* = 13.2, 9.0 Hz, 1H), 3.19–3.27 (m, 3H), 3.72–3.85 (m, 8H), 4.07–4.19 (m, 1H), 6.43 (s, 2H), 7.16 (d, *J* = 8.7 Hz, 1H), 7.31 (d, *J* = 8.1 Hz, 2H), 8.11 (d, *J* = 8.1 Hz, 2H); ^{13}C NMR ($CDCl_3$, 75 MHz) δ 28.3 (q), 30.6 (t), 34.9 (t), 36.2 (t), 37.0 (q), 51.7 (d), 55.4 (q), 55.8 (t), 63.5 (t), 80.9 (s), 98.4 (d), 103.9 (d), 119.1 (s), 123.6 (d), 129.2 (d), 131.2 (d), 146.3 (s), 150.0 (s), 158.8 (s), 160.2 (s), 170.9 (s). HRMS (Positive ion ESI) Calcd for $C_{26}H_{37}N_2O_7$ $[M - I + HO + H]^+$ *m/z* 489.5812. Found: $[M + H]^+$ *m/z* 489.2587.

2.4. *tert*-butyl 2-{[(2,4-dimethoxyphenyl)methyl][5-(4-nitrophenyl)-1-{4,7,10-tris[2-(*tert*-butoxy)-2-oxoethyl]-1,4,7,10-tetraazacyclododecan-1-yl}pentan-2-yl]amino}acetate (11)

To a solution of **8** (50 mg, 0.0907 mmol) in CH_3CN (5 mL) at 0 °C was added compound **10**[18] (46.66 mg, 0.0907 mmol) and DIPEA (23.43 mg, 0.181 mmol). The resulting mixture was stirred for 4 d at room temperature. The reaction mixture was concentrated to dryness *in vacuo*. The residue was sequentially washed with 0.1M HCl (10 mL) and 0.1M NaOH (10

mL). The resulting residue was concentrated to dryness *in vacuo* to provide pure **11** (65.4 mg, 73%). ^{1}H NMR ($CDCl_3$, 300 MHz) δ 1.39 (s, 36H), 1.50–2.09 (m, 4H), 2.52–2.95 (m, 14H), 3.05–4.70 (m, 17H), 3.77 (s, 6 H), 6.34–6.52 (m, 2H), 7.21 (d, J = 8.1 Hz, 1H), 7.40 (d, J = 8.4 Hz, 2H), 8.12 (d, J = 8.4 Hz, 2H). ^{13}C NMR ($CDCl_3$, 75 MHz) δ 28.1 (q), 28.2 (q), 28.6 (t), 29.6 (t), 35.8 (t), 48.6 (t), 51.0 (t), 51.6 (t), 51.8 (t), 53.3 (t), 55.3 (d), 55.5 (q), 55.6 (q), 56.3 (t), 56.9 (t), 81.3 (s), 81.3 (s), 81.4 (s), 81.6 (s), 98.4 (d), 104.8 (d), 118.1 (s), 123.6 (d), 129.3 (d), 130.6 (d), 146.4 (s), 150.0 (s), 158.8 (s), 160.7 (s), 170.3 (s), 170.6 (s), 171.1 (s). HRMS (Positive ion ESI) Calcd for $C_{52}H_{85}N_6O_{12}$ $[M + H]^+$ *m/z* 985.6220. Found: $[M + H]^+$ *m/z* 985.6224.

2.5. 2-{[5-(4-nitrophenyl)-1-[4,7,10-tris(carboxymethyl)-1,4,7,10-tetraazacyclododecan-1-yl]pentan-2-yl]amino}acetic acid (1)

To compound **11** (54 mg, 0.0548 mmol) was added 6M HCl solution (5 mL), and the resulting solution was refluxed for 15 min. The resulting solution was cooled to room temperature and washed with $CHCl_3$ (10 mL). The aqueous layer was concentrated and dried *in vacuo* to provide compound **1** (41 mg, 95%) present in a HCl salt as a waxy yellow solid. δ 1.40–1.79 (m, 4H), 2.41–4.01 (m, 29H), 7.32 (d, J = 8.1 Hz, 2H), 8.05 (d, J = 8.1 Hz, 1H). ^{13}C NMR (D_2O, 75 MHz) δ 25.5 (t), 27.8 (t), 34.3 (t), 45.2 (t), 49.1 (t), 49.8 (t), 50.9 (t), 52.4 (t), 52.7 (t), 54.2 (t), 54.8 (d), 55.7 (t), 123.6 (d), 129.4 (d), 145.8 (s), 150.0 (s), 168.9 (s). HRMS (Negative ion ESI) Calcd for $C_{27}H_{41}N_6O_{10}$ $[M - H]^-$ *m/z* 609.2890. Found: $[M - H]^-$ *m/z* 609.2926.

2.6. *tert*-butyl-2-{[2-bromo-5-(4-nitrophenyl)pentyl][(2,4-dimethoxyphenyl)methyl]-amino} acetate (12)

To a solution of **7** (300 mg, 0.614 mmol) and PPh_3 (193 mg, 0.737 mmol) in $CHCl_3$ (5 mL) at 0 °C was added portionwise NBS (131 mg, 0.737 mmol) over 5 min. The resulting mixture was stirred for 4 h at 0 °C. The ice bath was removed, and the reaction mixture was warmed to room temperature and stirred for 1 h. The solvent was evaporated, and the residue was purified by silica gel column chromatography eluted with 10% ethyl acetate in hexanes to afford **12** (210 mg, 63%) as a yellow oil.. ^{1}H NMR ($CDCl_3$, 300 MHz) δ 1.46 (s, 9H), 1.62–2.17 (m, 4H), 2.60–2.81 (m, 2H), 2.96 (dd, J = 13.8, 8.7 Hz, 1H), 3.17 (dd, J = 13.8, 5.4 Hz, 1H), 3.24 (s, 2H), 3.66–3.82 (m, 7H), 3.87 (d, J = 7.4 Hz, 1H), 3.94–4.12 (m, 1H), 6.40–6.46 (m, 2H), 7.15 (d, J = 9.0 Hz, 1H), 7.31 (d, J = 8.4 Hz, 2H), 8.12 (d, J = 8.7 Hz, 2H); ^{13}C NMR ($CDCl_3$, 75 MHz) δ 28.2 (q), 28.5 (t), 35.1 (t), 35.2 (t), 51.9 (t), 55.1 (d), 55.3 (q), 56.1 (t), 61.8 (t), 80.9 (s), 98.4 (d), 103.9 (d), 119.1 (s), 123.6 (d), 129.2 (d), 131.2 (d), 146.3 (s), 150.0 (s), 158.8 (s), 160.2 (s), 170.9 (s). HRMS (Positive ion ESI) Calcd for $C_{26}H_{35}N_2O_6$ $[M - Br]^+$ *m/z* 471.2490. Found: $[M - Br]^+$ *m/z* 471.2474.

2.7. tert-butyl 2-[(1-{4,7-bis[2-(tert-butoxy)-2-oxoethyl]-1,4,7-triazonan-1-yl}-5-(4-nitrophenyl)pentan-2-yl)[(2,4-dimethoxyphenyl)methyl]amino]acetate (15)

To a solution of **12** (50 mg, 0.0907 mmol) in CH_3CN (1 mL) at −5 °C was added $AgClO_4$ (18.8 mg, 0.0907 mmol). The resulting mixture was stirred for 10 min at the same temperature. Compound **14**[15] (32.4 mg, 0.0907 mmol) and DIPEA (35.2 mg, 0.272 mmol) was sequentially added to the reaction mixture at −5 °C. The resulting mixture was

gradually warmed to room temperature and stirred for 20 h. The reaction mixture was filtered and concentrated to the dryness *in vacuo*. 0.1M HCl solution (10 mL) was added to the residue, and the resulting mixture was extracted with CH_2Cl_2 (3 × 10 mL). The combined organic layers were dried over $MgSO_4$, filtered, and concentrated *in vacuo*. The residue was purified via column chromatography on silica gel (60–220 mesh) sequentially eluted with 50 % ethyl acetate in hexanes and then with 3% CH_3OH in CH_2Cl_2 to provide pure product **15** (70 mg, 80%) as a yellowish oil. ^{1}H NMR ($CDCl_3$, 300 MHz) δ 1.29–1.48 (m, 27H), 1.50–1.94 (m, 4H), 2.61–3.93 (m, 31H), 6.34–6.45 (m, 2H), 7.05 (d, J = 8.1 Hz, 1H), 7.38 (d, J = 7.8 Hz, 2H), 8.09 (d, J = 7.8 Hz, 2H). ^{13}C NMR ($CDCl_3$, 75 MHz) δ 27.3 (t), 28.0 (q), 28.1 (q), 28.4 (t), 35.8 (t), 50.0 (t), 50.8 (t), 51.4 (t), 51.9 (t), 54.0 (t), 54.4 (t), 55.4 (q), 56.9 (d), 57.4 (t), 58.5 (t), 58.7 (t), 81.5 (s), 81.6 (s), 82.1 (s), 98.6 (d), 104.4 (d), 117.7 (s), 123.6 (d), 129.5 (d), 131.9 (d), 146.3 (s), 149.8 (s), 158.8 (s), 160.8 (s), 170.5 (s), 170.6 (s), 173.1 (s). HRMS (Positive ion ESI) Calcd for $C_{44}H_{70}N_5O_{10}$ $[M + H]^+$ *m/z* 828.5117. Found: $[M + H]^+$ *m/z* 828.5161.

2.8. 2-({1-[4,7-bis(carboxymethyl)-1,4,7-triazonan-1-yl]-5-(4-nitrophenyl)pentan-2-yl} amino)acetic acid (2)

To compound **15** (67 mg, 0.0809 mmol) was added 6M HCl solution (3 mL), and the resulting solution was maintained at reflux for 15 min. The reaction was allowed to room temperature, and the resulting solution was filtered and dried *in vacuo* to provide the desired chelate **2** (51 mg, 96%) as a waxy yellow solid. ^{1}H NMR (D_2O, 300 MHz) δ 1.38–1.70 (m, 4H), 2.47–3.36 (m, 16H), 3.27–3.40 (m, 1H), 3.67–3.91 (m, 6H), 7.27 (d, J = 7.8 Hz, 2H), 7.96 (d, J = 7.8 Hz, 1H). ^{13}C NMR (D_2O, 75 MHz) δ 25.6 (t), 27.1 (t), 34.6 (t), 44.5 (t), 49.1 (t), 49.6 (t), 51.9 (t), 55.6 (d), 56.0 (t), 59.0 (t), 123.9 (d), 129.6 (d), 146.1 (s), 150.3 (s), 169.1 (s), 172.0 (s). HRMS (Positive ion FAB) Calcd for $C_{23}H_{36}N_5O_8$: $[M + H]^+$ *m/z* 510.2558. Found: $[M + H]^+$ *m/z* 510.2557.

2.9. 1,3-diethyl 2-[3-(4-nitrophenyl)propyl]propanedioate (17).[19]

To a round bottom flask containing 60% NaH in mineral oil (272 mg, 6.80 mmol) in an ice-bath was added THF (10 mL). A solution of diethyl malonate (1.04 g, 6.47 mmol) in THF (10 mL) was added dropwise over 10 min at 0 °C, and the reaction mixture was stirred for 30 min. To the reaction mixture was added dropwise a solution of **16**[16] (1.58 g, 6.47 mmol) in THF (10 mL) over 10 min. The reaction was warmed to room temperature and stirred for 1 d. The reaction mixture was quenched by H_2O (10 mL) and evaporated to dryness. H_2O (30 mL) was added to the mixture, and the resulting solution was extracted with ethyl acetate (3 × 30 mL). The combined organic layers were dried over $MgSO_4$ and concentrated to the dryness *in vacuo*. The residue was purified via column chromatography on silica gel (60–220 mesh) eluted with 8% ethyl acetate in hexanes to afford pure **17** (1.46 g, 70%) as a light yellow oil. ^{1}H NMR ($CDCl_3$, 300 MHz) δ 1.23 (t, J = 7.2 Hz, 6H), 1.61–1.79 (m, 2H), 1.83–1.98 (m, 2H), 2.74 (t, J = 7.5 Hz, 2H), 3.32 (t, J = 7.2 Hz, 1H), 4.07–4.25 (m, 4H), 7.31 (d, J = 8.4 Hz, 2H), 8.11 (d, J = 8.7 Hz, 2H); ^{13}C NMR ($CDCl_3$, 75 MHz) δ 14.1 (q), 28.1 (t), 28.5 (t), 35.4 (t), 51.7 (d), 61.4 (t), 123.7 (d), 129.2 (d), 146.4 (s), 149.5 (s), 169.2 (s).

2.10. 5-(4-nitrophenyl)pentanoic acid (18).[20]

Compound **17** (2.5 g, 7.7 mmol) was dissolved in the mixture of acetic acid (20 mL) and conc. HCl (20 mL), and the resulting solution was refluxed for 24 h. The reaction mixture was cooled to room temperature and concentrated *in vacuo* to provide **18** (1.6 g, 93.2%) as a yellow solid that was used for the next step without further purification. ^{1}H NMR (D_2O + NaOD, 300 MHz) δ 1.29–1.42 (m, 4H), 1.97–2.07 (m, 2H), 2.38–2.49 (m, 2H), 7.06 (d, J = 8.4 Hz, 2H), 7.71 (d, J = 8.4 Hz, 2H); ^{13}C NMR (D_2O, 75MHz) δ 25.5 (t), 30.1 (t), 34.8 (t), 37.3 (t), 123.3 (d), 129.1 (d), 145.3 (s), 151.6 (s), 183.4 (s).

2.11. methyl 2-bromo-5-(4-nitrophenyl)pentanoate (19).[20]

Compound **18** (500 mg, 2.24 mmol) was added to a solution of CCl_4 (0.5 ml) and thionyl chloride (1.07 g, 8.97 mmol). The solution was brought to reflux for 1 h. At this point, NBS (598.1 mg, 3.36 mmol) was added, and 1 drop of 48% aqueous HBr catalyst was added to the warm solution. The dark solution was refluxed for an additional 1 h and became clear. The solution was cooled, and MeOH (7 mL) was added with stirring. The excess solvent was removed and gave a mixture of yellowish oil (60:40). The residue was purified via column chromatography on silica gel (60–220 mesh) eluting 50% CH_2Cl_2 in hexane afford pure **19** (414 mg, 58.4%) as a colorless oil. ^{1}H NMR ($CDCl_3$, 300 MHz) δ 1.61–1.89 (m, 2H), 1.96–2.06 (m, 2H), 2.72 (t, J = 7.5 Hz, 2H), 3.72 (s, 3H), 4.22 (t, J = 7.2 Hz, 1H), 7.29 (d, J = 8.7 Hz, 2H), 8.07 (d, J = 8.7 Hz, 2H); ^{13}C NMR ($CDCl_3$, 75 MHz) δ 28.4 (t), 34.1 (t), 34.8 (t), 45.2 (d), 53.0 (t), 123.7 (d), 129.2 (d), 146.4 (s), 149.3 (s), 170.0 (s).

2.12. Methyl 2-{4,7-bis[2-(tert-butoxy)-2-oxoethyl]-1,4,7-triazonan-1-yl}-5-(4-nitrophenyl) pentanoate (20)

Compound **19** (50 mg, 0.158 mmol) was added dropwise to a solution of **14** (56.5 mg, 0.158 mmol) in CH_3CN (0.5 mL) at 0 °C. DIPEA (61.1 mg, 0.474 mmol) in CH_3CN (0.5 mL) was added dropwise. The resulting mixture was allowed to room temperature and stirred for 5 d, while monitoring the reaction progress using TLC. After which period of time, the reaction mixture was evaporated to dryness. The residue was dissolved with 0.1M HCl solution (10 mL) and washed with $CHCl_3$ (2 × 10 mL). The combined organic layers were dried over $MgSO_4$, filtered, and concentrated to the dryness *in vacuo*. The residue was purified via column chromatography on silica gel (60–220 mesh) and eluted with 10% MeOH in CH_2Cl_2 to provide pure **20** (92 mg, 98%) as a yellow oil. ^{1}H NMR ($CDCl_3$, 300 MHz) δ 1.43 (s, 9H), 1.60–1.94 (m, 4H), 2.65–3.03 (m, 14H), 3.28 (s, 5H), 3.65 (s, 3H), 7.33 (d, J = 8.4 Hz, 2H), 8.12 (d, J = 8.4 Hz, 2H); ^{13}C NMR ($CDCl_3$, 75 MHz) δ 27.9 (t), 28.2 (q), 30.0 (t), 35.6 (t), 51.0 (q), 53.5 (t), 55.2 (t), 55.9 (t), 59.4 (t), 66.8 (d), 80.7 (s), 123.6 (d), 129.2 (d), 146.4 (s), 150.1 (s), 171.4 (s), 174.0 (s). HRMS (positive ion ESI) Calcd for $C_{30}H_{49}N_4O_8$ $[M + H]^+$ m/z 593.3545. Found: $[M + H]^+$ m/z 593.3529.

2.13. 2-[4,7-bis(carboxymethyl)-1,4,7-triazonan-1-yl]-5-(4-nitrophenyl)pentanoic acid (3)

To compound **20** (55 mg, 0.0928 mmol) was added 6M HCl solution (6 mL), and the resulting solution was maintained at reflux for 3 h. The reaction was allowed to room temperature, and the resulting solution was filtered through Celite® using 18Ω H_2O and dried *in vacuo* to provide compound **3** (47.7 mg, 89.3%) as a yellow solid. ^{1}H NMR (D_2O,

300 MHz) δ 1.50–1.79 (m, 4H), 2.49–2.62 (m, 2H), 2.99–3.05 (m, 12H), 3.58–3.67 (m, 1H), 3.70–3.92 (m, 4H), 7.16 (d, J = 8.1 Hz, 2H), 7.83 (d, J = 8.1 Hz, 2H); ^{13}C NMR (D_2O, 75 MHz) δ 27.3 (t), 27.7 (t), 34.7 (t), 45.7 (t), 47.2 (t), 50.1 (t), 51.0 (t), 55.8 (t), 65.3 (d), 123.6 (d), 129.5 (d), 145.9 (s), 150.5 (s), 171.5 (s), 174.4 (s). HRMS (positive ion ESI) Calcd for $C_{21}H_{29}N_4O_8$ $[M - H]^+$ *m/z* 465.1991. Found: $[M - H]^+$ *m/z* 465.1999.

2.14. Radiolabeling of the bifunctional chelates with ^{90}Y and ^{177}Lu

All HCl solutions were prepared from ultra pure HCl (JT baker, #6900-05). For metal-free radiolabeling, plasticware including pipette tips, tubes, and caps was soaked in 0.1M HCl (aq) overnight and washed thoroughly with 18 MΩ water, and air-dried overnight. Ultra pure ammonium acetate (Aldrich, #372331) was purchased from Aldrich and used to prepare buffer solutions (0.25 M) at various pHs. After adjusting pH using 0.1M HCl or 0.1M NaOH solution, 0.25 M NH_4OAc buffer solutions were treated with Chelex-100 resin (Biorad, #142-2842, 1g/100ml buffer solution), shaken overnight at room temperature, and filtered through 0.22 μM filter (Corning, #430320) prior to use. ^{90}Y and ^{177}Lu were purchased from Perkin Elmer. TLC plates (6.6 × 1 cm, Silica gel 60 F_{254}, EMD Chemicals Inc., #5554-7) with the origin line drawn at 0.6 cm from the bottom were prepared.

To a buffer solution (0.25M NH_4OAc, pH 5.5 or pH 7.0) in a capped microcentrifuge tube (1.5 mL, #05-408-129) was sequentially added a solution of a chelate in water (20 μg) and ^{90}Y or ^{177}Lu (60 μCi). The total volume of the resulting solution was 40 μL. The reaction mixture was agitated on the thermomixer (Eppendorf, #022670549) set at 1,000 rpm at room temperature for 1 h. The labeling efficiency was determined by ITLC eluted with CH_3CN/H_2O (3:2 v/v) or 20 mM EDTA in 0.15 M NH_4OAc as the mobile phase. A solution of radiolabeled complexes (2 μL) was withdrawn at the designated time points (1 min, 10 min, 20 min, 30 min, and 60 min), spotted on a TLC plate, and then eluted with the mobile phase. After completion of elution, the TLC plate was warmed and dried on the surface of a heater maintained at 35 °C and scanned using TLC scanner (Bioscan, #FC-1000). Unbound (R_f = 0.6) and bound (R_f = 0.9) radioisotope appeared around 30 mm and 50 mm from the bottom of the TLC plate eluted with CH_3CN/H_2O (3:2 v/v), respectively. For the ITLC eluted with 20 mM EDTA in 0.15 M NH_4OAc system, unbound (R_f = 0.9) and bound (R_f = 0.6) radioisotope appeared around 50 mm and 30 mm, respectively.

2.15. *In vitro* serum stability of ^{90}Y- and ^{177}Lu-radiolabeled complexes

Human serum was purchased from Gemini Bioproducts (#100110). ^{90}Y- or ^{177}Lu-radiolabeled complexes (0.25M NH_4OAc, pH 5.5) were prepared from the reaction of chelates with ^{90}Y or ^{177}Lu at room temperature or 37 °C. Completion of radiolabeling was monitored by ITLC eluted, and the freshly prepared radiolabeled complexes were used for serum stability without further purification. ^{90}Y-3p-*C*-DE4TA, ^{90}Y-3p-*C*-NE3TA and ^{90}Y-3p-*C*-NOTA were prepared by a reaction of 3p-*C*-DE4TA (**1**), 3p-*C*-NE3TA (**2**) and 3p-*C*-NOTA (**3**) (50 μg) with ^{90}Y (150 μCi) in 0.25 M NH_4OAc buffer (pH 7.0). Radiolabeling of 3p-*C*-DE4TA, 3p-*C*-NE3TA and 3-*C*-NOTA with ^{90}Y were complete in 2 h at 37 °C (600 rpm). ^{90}Y-3p-*C*-DEPA (4) was prepared by a reaction of 3p-*C*-DEPA (100 μg, 100 μL) with ^{90}Y (300 μCi) in 0.25 M NH_4OAc buffer (pH 5.5). Radiolabeling of 3p-*C*-

DEPA with ^{90}Y was complete in 4 h at RT (1000 rpm) and 2 h at 37 °C (300 rpm). The complexes ^{90}Y-3p-*C*-DE4TA, ^{90}Y-3p-*C*-NE3TA, ^{90}Y-3-*C*-NOTA, and ^{90}Y-3p-*C*-DEPA prepared from the reactions were directly used for serum stability studies without further purification. ^{90}Y-3p-*C*-DE4TA (144 μCi, 99 μL), ^{90}Y-3p-*C*-NE3TA (144 μCi, 99 μL), or ^{90}Y-3-*C*-NOTA (144 μCi, 99 μL) was added to human serum (500 μL) in a microcentrifuge tube. ^{90}Y-3p-*C*-DEPA (90 μCi, 63 μL) was added to human serum (330 μL) in a microcentrifuge tube. ^{177}Lu-3p-*C*-DE4TA, ^{177}Lu-3p-*C*-NE3TA, ^{177}Lu-3-*C*-NOTA, and ^{177}Lu-3p-*C*-DEPA were prepared by a reaction of 3p-*C*-DE4TA, 3p-*C*-NE3TA, 3p-*C*-NOTA, 3p-*C*-DEPA (50 μg) with ^{177}Lu (150 μCi) in 0.25M NH_4OAc buffer (pH 5.5), respectively. Radiolabeling of 3p-*C*-DE4TA and 3p-*C*-DEPA with ^{177}Lu was complete in 3 h at room temperature and 1000 rpm. Radiolabeling of 3p-*C*-NE3TA and 3p-*C*-NOTA with ^{177}Lu was complete in 2 h at room temperature and 1000 rpm. The complexes ^{177}Lu-3p-*C*-DE4TA, ^{177}Lu-3p-*C*-DEPA, ^{177}Lu-3p-*C*-NE3TA, and ^{177}Lu-3-*C*-NOTA prepared from the reactions were directly used for serum stability studies without further purification. ^{177}Lu-3p-*C*-DE4TA (146 μCi, 100 μL), ^{177}Lu-3p-*C*-DEPA (146 μCi, 100 μL), ^{177}Lu-3p-*C*-NE3TA (149 μCi, 100 μL), or ^{177}Lu-3-*C*-NOTA (149 μCi, 100 μL) was added to human serum (500 μL) in a microcentrifuge tube. The stability of the radiolabeled complexes in human serum was evaluated at 37 °C over 14 days. The serum stability of the radiolabeled complexes was assessed by measuring the transfer of the radionuclide from each complex to serum proteins using ITLC eluted with CH_3CN/H_2O (3:2 v/v) or 20mM EDTA in 0.15M NH_4OAc. A solution of the radiolabeled complex in serum was withdrawn at the designated time point, and the percentage of ^{90}Y or ^{177}Lu released from each of the radiolabeled complexes into serum was assessed by ITLC as described above.

2.16. Biodistribution Studies

All animal experiments were conducted in accordance with the guidelines established by the Animal Care and Use Committee of the University of Missouri and the Harry S. Truman Memorial Veterans' Hospital Subcommittee for Animal Studies. Six to eight week old CF-1 mice were obtained from Charles River Laboratories and housed one week prior to the studies. An aliquot of each ^{177}Lu-radiolabeled complex (60 μCi) that was prepared as described above were intravenously injected via the tail vein in a volume of 100 μL of phosphate-buffered saline. At 1 h, 4 h and 24 h post-injection, mice were sacrificed and blood, liver, kidney, muscle and bone were collected, weighed and counted in a gamma counter. The radioactivity from each tissue/organ was decay-corrected by a known aliquot of the injected dose, and the percent-injected dose per gram of tissue (% ID/g) was calculated. Values were presented as mean ± SD for each group of 3 mice.

3. Results and Discussion

Synthesis

3p-*C*-DE4TA (**1**) contains a 12-membered larger macrocyclic backbone, while heptadentate 3p-*C*-NE3TA (**2**) is structured on a smaller triazacyclononane (TACN) ring. Both 3p-*C*-DE4TA and 3p-*C*-NE3TA possess a less hindered bidentate acyclic pendant arm relative to 3p-*C*-DEPA (**4**) and 3p-*C*-NETA (**5**), respectively. Hexadentate 3p-*C*-NOTA (**3**) does not

have the flexible pendant arm required for bimodal binding by cooperation of acyclic and macrocyclic binding moieties and was designed to compare the effect of bimodality on complexation with the radiolanthanides. The new bifunctional chelates 3p-*C*-DE4TA (**1**) and 3p-*C*-NE3TA (**2**) as shown in Schemes 1 and 2 were prepared based on the regiospecific ring opening of labile aziridinium ions (**9** and **13**) with a prealkylated macrocycle DO3A (tri-*tert*-butyl 1,4,7,10-tetraazacyclododecane-1,4,7-triacetate **10**) and NO2A (di-*tert*-butyl-1,4,7-triazacyclononane-1,4-diacetate, **14**). Synthesis of 3p-*C*-DE4TA is outlined in Scheme 1. Reductive amination of amino alcohol **5**[16] with dimethoxybenzaldehyde provided *N*-dimethoxybenzyl (DMB) protected compound **6** which was further alkylated to afford bi-substituted amino alcohol **7**. Halogenation of **7** using I_2 and PPh_3 afforded secondary β-amino iodide **8.** Conversion of **8** to aziridinium ion **9** followed by nucleophilic reaction of **9** with trialkylated macrocyclic cyclen **10**[18] at the less hindered carbon provided the desired ring opening product **11** as the regiospecific isomer. Subsequent removal of the *tert*-butyl and DMB groups in **11** by treatment of **11** with 6M HCl(aq) under reflux provided 3p-*C*-DE4TA (**1**) in quantitative yield. Synthesis of 3p-*C*-NE3TA (**2**) is outlined in Scheme 2. Reaction of **7** with brominating agent (NBS and PPh_3) afforded secondary β-amino bromide **12.** Intramolecular rearrangement of β-bromoamine **12** to aziridinium ion **13** was promoted by halogen sequestering agent ($AgClO_4$). Reaction of NO2A (**14**)[15] with the alkylating agent **13** provided the nucleophilic ring opening product **15** as the regiospecific isomer. Compound **15** was subjected to acidic hydrolysis using HCl(aq) for removal of the protective *tert*-butyl groups in **15**. Synthesis of 3p-*C*-NOTA is shown in Scheme 3. A basepromoted reaction of *p*-nitrophenylpropyl bromide (**16**)[16] with diethyl malonate provided compound **17** which was subsequently subjected to hydrolysis to afford a functionalized carboxylic acid **18**. Chlorination of **18** followed by α-bromination and esterification afforded α-bromomethyl ester **19**.[20] Subsequent reaction of **19** with bisubstituted TACN **14**[15] provided compound **20** which was treated with 6M HCl(aq) to produce 3p-*C*-NOTA (**3**).

Radiolabeling kinetics and *in vitro* serum stability

We previously reported 3p-*C*-NETA (**5**) instantly bound to ^{90}Y or ^{177}Lu (1 min, >99% radiolabeling efficiency).[16] *C*-DOTA was slower than 3p-*C*-NETA in binding both ^{90}Y and ^{177}Lu.[16] Both ^{90}Y- and ^{177}Lu-radiolabeled 3p-*C*-NETA and *C*-DOTA complexes remained stable in human serum for 2 weeks without releasing any measurable radioactivity.[16] 3p-*C*-NETA was used as a positive control for radiolabeling kinetics and serum stability studies as previously reported.[16] The bifunctional chelates 3p-*C*-DE4TA (**1**), 3p-*C*-NE3TA (**2**), 3p-*C*-NOTA (**3**), and 3p-*C*-DEPA (**4**)[17] were evaluated for radiolabeling efficiency with ^{90}Y and ^{177}Lu (Tables 1 and 2 and supporting information). A chelate (20 μg) in 0.25M NH_4OAc buffer solution was radiolabeled with ^{90}Y or ^{177}Lu (60 μCi) at room temperature (RT). During the reaction time (1 h), the radiolabeling kinetics was determined using ITLC. Radiolabeling of 3p-*C*-DE4TA (**1**) with ^{90}Y or ^{177}Lu was nearly complete at 10 min time point (>99% radiolabeling efficiency, pH 7). It should be noted that 3p-*C*-DE4TA (**1**) was very slow in binding both ^{90}Y and ^{177}Lu at pH 5.5 (1 min, 7% and 21% radiolabeling efficiency for ^{90}Y and ^{177}Lu, respectively, Supporting Information). It is speculated that the protonated secondary amine in the chelate may not participate in

complexation under acidic condition and lead to slow radiolabeling of the chelate. A dramatic increase in radiolabeling kinetics was observed when 3p-*C*-DE4TA (**1**) was subjected to radiolabeling at pH 7 (1 min, >85% radiolabeling efficiency for ^{90}Y and ^{177}Lu). Both 3p-*C*-NE3TA (**2**) and 3p-*C*-NOTA (**3**) were more sluggish in binding ^{90}Y than ^{177}Lu. 3p-*C*-NE3TA and 3p-*C*-NOTA bound to ^{90}Y with the respective radiolabeling efficiencies of 69% and 89% at the 1 h time point, while radiolabeling of 3p-*C*-NE3TA and 3p-*C*-NOTA with the smaller metal cation ^{177}Lu was nearly complete at 1 h time point. When compared to 3p-*C*-NETA (**5**) with the same macrocyclic cavity, 3p-*C*-NE3TA (**2**) and 3p-*C*-NOTA (**3**) were significantly slower in binding ^{90}Y and ^{177}Lu, although the chelates were more efficient in binding the metals at pH 7 (Supporting Information). This result clearly demonstrates that the tridentate acyclic moiety is critical in enhancing complexation kinetics via bimodal binding. It is interesting to note that hexadentate 3p-*C*-NOTA was more efficient in binding both ^{90}Y and ^{177}Lu than 3p-*C*-NE3TA, although 3p-*C*-NOTA has an insufficient number of donor groups for complex with the large metal cations. Decadendate 3p-*C*-DEPA (**4**) rapidly sequestered ^{90}Y and ^{177}Lu with the respective radiolabeling efficiency of 89% and 94% at 1 min time point. 3p-*C*-DE4TA (**1**) and 3p-*C*-DEPA (**4**) with the same macroyclic cavity displayed similar complexation kinetics with the metals.

^{90}Y- or ^{177}Lu-radiolabeld chelates were further evaluated for *in vitro* serum stability (n = 2, Figures 2 and 3 and Supporting Information). ^{90}Y-3p-*C*-DE4TA (**1**) was found to be stable in serum for at least for 2 weeks, while a small amount of ^{177}Lu (~5%) was lost from ^{177}Lu-3p-*C*-DE4TA (**1**) over 2 weeks. A significant amount of the radioactivity from both ^{90}Y-3p-*C*-DEPA (**4**) and ^{177}Lu-3p-*C*-DEPA (**4**) was transchelated to serum (25% and 45% in 72 h, respectively). As expected,[10–11] both ^{90}Y and ^{177}Lu complexes of 3p-*C*-NOTA (**3**) were not stable in serum, and ~80% of ^{90}Y and ~36% of ^{177}Lu was released from the complexes on day 7. The result indicate that NOTA rapidly can form a kinetically labile complex that is instantly dissociated in serum. ^{177}Lu-3p-*C*-NE3TA (**2**) remained quite stable in serum, and only ~4% of the radioactivity was transferred from the complex to serum. However, ^{90}Y-3p-*C*-NE3TA underwent rapid dissociation, losing ~25% of ^{90}Y to serum in 2 days. It appears that heptadentate chelate 3p-*C*-NE3TA failed to tightly hold the larger metal, ^{90}Y due to an insufficient number of donors, while 3p-*C*-NE3TA can form a complex with the smaller metal ^{177}Lu with enhanced complex stability. The radiolabeling and serum stability data indicate that decadentate chelate 3p-*C*-DEPA (4) instantly bound to ^{90}Y and ^{177}Lu, but failed to hold ^{90}Y or ^{177}Lu in serum. It seems that the DEPA built on the larger macrocyclic cavity has too many donor groups to form a stable complex with the relatively smaller metal cations Y(III) and Lu(III), and this excessive ligand denticity may promote formation and dissociation of the Lu(III)- or Y(III)-DEPA complex in equilibrium. It should be noted that DE4TA and DEPA are structured on the same cyclen-based ring and display completely different complex stability with Y(III) and Lu(III). The comparative data of 3p-*C*-DE4TA (**1**) and 3p-*C*-DEPA (**4**) suggest that denticity in the chelates with the large macrocyclic cavity plays a critical role in complexation. 3p-*C*-DE4TA with 9 donors were significantly more effective than 3p-*C*-DEPA with 10 donors in complexing ^{90}Y. No substantial difference in complexation of ^{90}Y between 3p-*C*-DE4TA (**1**) and 3p-*C*-NETA (**5**), the standard gold chelate, was observed. It appears that the nine donor groups on the large cyclen ring of the nonadentate DE4TA were well tolerated to complex with ^{90}Y with

high complexation kinetics and stability. The slightly enhanced complex stability observed with ^{90}Y-3p-*C*-DE4TA relative to ^{177}Lu-3p-*C*-DE4TA may be explained by a better size-match between the cavity and the larger metal Y(III) that is well balanced with the nine donor groups. It seems that 3p-*C*-DE4TA with the larger macrocyclic cavity have too many donors to hold smaller Lu(III) with high complex stability. The effect of the size-match was also demonstrated from evaluation of 3p-*C*-NE3TA (**2**) and 3p-*C*-NOTA (**3**). 3p-*C*-NE3TA with the small cavity, was completely ineffective in complexing the larger metal cation Y(III) with high stability, while Lu(III) was quite tightly chelated with 3p-*C*-NE3TA. It is demonstrated that 3p-*C*-NOTA (**3**) was incapable of chelating the lanthanides effectively due to the poor size match. It is noteworthy that replacement of the bidentate amiocaroxylate group in the NOTA with a more flexible tridentate group led to enhanced complex stability with ^{177}Lu as shown in complexation of the NE3TA. This result clearly demonstrate that the pendant acyclic donors are essential in effective complexation with the metals, and the improved complexation kinetics and stability of other bimodal chelates as compared to the NOTA, predominantly resulted from cooperative and bimodal binding of acyclic and macrocyclic donors. The comparative complexation kinetic and stability data indicate that a well-coordinated interplay of bimodality, cavity size, and ligand denticity is critical for the dynamic and tight binding of the bimodal chelates with a metal. Octadentate 3p-*C*-NETA with the smaller 9-membered ring was shown to be the most effective chelate in binding the lanthanides. The nanodentate chelate (3p-*C*-DE4TA) with the larger macrocyclic cavity formed a metal complex with the larger metal ^{90}Y with fast radiolabeling kinetics and high complex stability. The heptadentate chelate (3p-C-NE3TA) with the smaller 9-membered ring bound to the smaller metal ^{177}Lu in a decent level of complexation kinetics and stability.

In vivo biodistribution

The *in vivo* stability of ^{177}Lu-radiolabeled complexes of two promising chelates 3p-*C*-DE4TA (**1**) and 3p-*C*-NE3TA (**2**) was evaluated by performing biodistribution studies in CF-1 normal mice (i.v. injection, n = 3). 3p-*C*-NETA (**5**) as a positive control was also evaluated for *in vivo* biodistribution for comparison. The mice were euthanized at 1 h, 4 h, and 24 h. Selected organs and blood were harvested, weighed, and the radioactivity was measured in a γ-counter (Figure 4 and Supporting Information). As expected, 3p-*C*-NETA used as a positive control displayed excellent *in vivo* complex stability as demonstrated by the low radioactivity level in the blood and organs at all time points studied. A very low radioactivity level in the blood (<0.5% ID/g) was observed with the ^{177}Lu-radiolabeled complexes at all of the time points studied. Among the organs, the highest accretion of radioactivity was observed in the liver at 1 h time point (6.7% ID/g for ^{177}Lu-3p-*C*-DE4TA, 1.4% ID/g for ^{177}Lu-3p-*C*-NETA, and 17.2% ID/g for ^{177}Lu-3p-*C*-NE3TA). ^{177}Lu-3p-*C*-NE3TA exhibited a 3-fold higher retention in the liver as compared to ^{177}Lu-3p-*C*-DE4TA at 1 h post-injection, although the NE3TA complex exhibited negligible accumulation of radioactivity in the liver at 24 h. All of the ^{177}Luradiolabeled complexes displayed low radioactivity accumulation in bone and muscle, which peaked at 1 h (<0.5% ID/g) and decreased by 24 h (<0.1% ID/g). The highest renal retention at the 1 h time point (5.5% ID/g) was observed with ^{177}Lu-3p-*C*-NE3TA, while ^{177}Lu-3p-*C*-DE4TA displayed a very low uptake in the kidney (<0.6% ID/g) at all of the time points studied.

4. Conclusion

The new bifunctional chelates 3p-*C*-DE4TA (**1**), 3p-*C*-NE3TA (**2**), and 3p-*C*-NOTA (**3**) were prepared and evaluated for complexation with ^{90}Y and ^{177}Lu. The known bimodal chelates 3p-*C*-DEPA (**4**) and 3p-*C*-NETA (**5**) with different coordination chemistry were evaluated for comparison. 3p-*C*-DE4TA (**1**) was shown to rapidly produce ^{90}Y- or ^{177}Lu-radiolabeled complexes at room temperature. The serum stability data indicate that ^{90}Y and ^{177}Lu-radiolabeled complexes of 3p-*C*-DE4TA (**1**) displayed excellent to good complex stability in serum. 3p-*C*-NE3TA (**2**) with a smaller macrocyclic cavity and lower denticity than 3p-*C*-DE4TA (1) was slower in binding ^{90}Y or ^{177}Lu. ^{177}Lu-3p-*C*-NE3TA (**2**) remained quite inert in serum, while ^{90}Y- 3p-*C*-NE3TA (**2**) was gradually dissociated in serum. The bifunctional version of NOTA (3p-*C*-NOTA) was shown to be ineffective in binding ^{90}Y and ^{177}Lu. The results of the comparative complexation kinetic and stability studies indicate that bimodality, cavity size, and ligand denticity have an impact on complexation of the bifunctional chelates with the radiolanthanides, and a well-coordinated interplay of the factors is critical for the dynamic and tight binding of the bifunctional chelates with ^{90}Y and ^{177}Lu. In summary, 3p-*C*-DE4TA (**1**) and 3p-*C*-NE3TA (**2**) are promising bifunctional chelates of ^{90}Y and ^{177}Lu and will be further evaluated for antibody-targeted radiotherapy of cancer.

Supplementary Material

Refer to Web version on PubMed Central for supplementary material.

Acknowledgments

We acknowledge the financial support from the National Institutes of Health (2R01CA112503 to H. S. Chong). We also thank the Department of Veterans Affairs, for providing resources and use of facilities at the Harry S. Truman Memorial Veterans' Hospital in Columbia, MO.

References and Notes

1. Milenic DE, Brady ED, Brechbiel MW. Nature Rev. 2004; 3:488–498.
2. Srivastava S, Dadachova E. Semin Nucl Med. 2001; 31:330–341. [PubMed: 11710775]
3. Knox SJ, Meredith RF. Sem Radiat Oncol. 2000; 10:73–93.
4. Wiseman GA, White CA, Sparks RB, Erwin WD, Podoloff DA, Lamonica D, Bartlett NL, Parker JA, Dunn WL, Spies SM, Belanger R, Witzig TE, Leigh BR. Crit Rev Oncol Hematol. 2001; 39:181–194. [PubMed: 11418315]
5. Parker D. Chem Soc Rev. 1990; 19:271–291.
6. Brechbiel MW. Q J Nucl Med Mol Imaging. 2008; 52:166–173. [PubMed: 18043537]
7. Shannon RD. Acta Crys. 1976; A32:751–767.
8. Hancock RD, Martell AE. Chem Rev. 1989; 89:1875–1914.
9. Alexander V. Chem Rev. 1995; 95:273–342.
10. Brucher E, Sherry AD. Inorg Chem. 1990; 29:1555–1559.
11. Cacheris WP, Nickle SK, Sherry AD. Inorg Chem. 1987; 26:958–960.
12. Chong HS, Sun X, Dong P, Kang CS. Eur J Org Chem. 2011; 33:6641–6648.
13. Chappell LL, Ma D, Milenic DE, Garmasteni K, Venditto V, Beitzel MP, Brechbiel MW. Nucl Med Biol. 2003; 30:581–595. [PubMed: 12900284]

14. Kang CS, Sun X, Jia F, Song HA, Chen Y, Lewis M, Chong HS. Bioconjugate Chem. 2012; 23:1775–1782.
15. Chong HS, Song HA, Birch N, Le T, Lim SY, Ma X. Bioorg Med Chem Lett. 2008; 18:3436–3439. [PubMed: 18445528]
16. Chong HS, Song HA, Kang CS, Le T, Sun X, Dadwal M, Lee HB, Lan X, Chen Y, Dai A. Chem Commun. 2011; 47:5584–5586.
17. Song HA, Kang CS, Baidoo KE, Milenic DE, Chen Y, Dai A, Brechbiel MW, Chong HS. Bioconjugate Chem. 2011; 22:1128–1135.
18. Chong HS, Lim S, Baidoo KE, Milenic DE, Ma X, Jia F, Song HA, Brechbiel MW, Lewis MR. Bioorg Med Chem Lett. 2008; 18:5792–5795. [PubMed: 18845437]
19. Citterio A, Fancelli D, Finzi C, Pesce L, Santi R. J Org Chem. 1989; 54:2713–2718.
20. Kline SJ, Betebenner DA, Johnson DK. Bioconjugate Chem. 1991; 2:26–31.

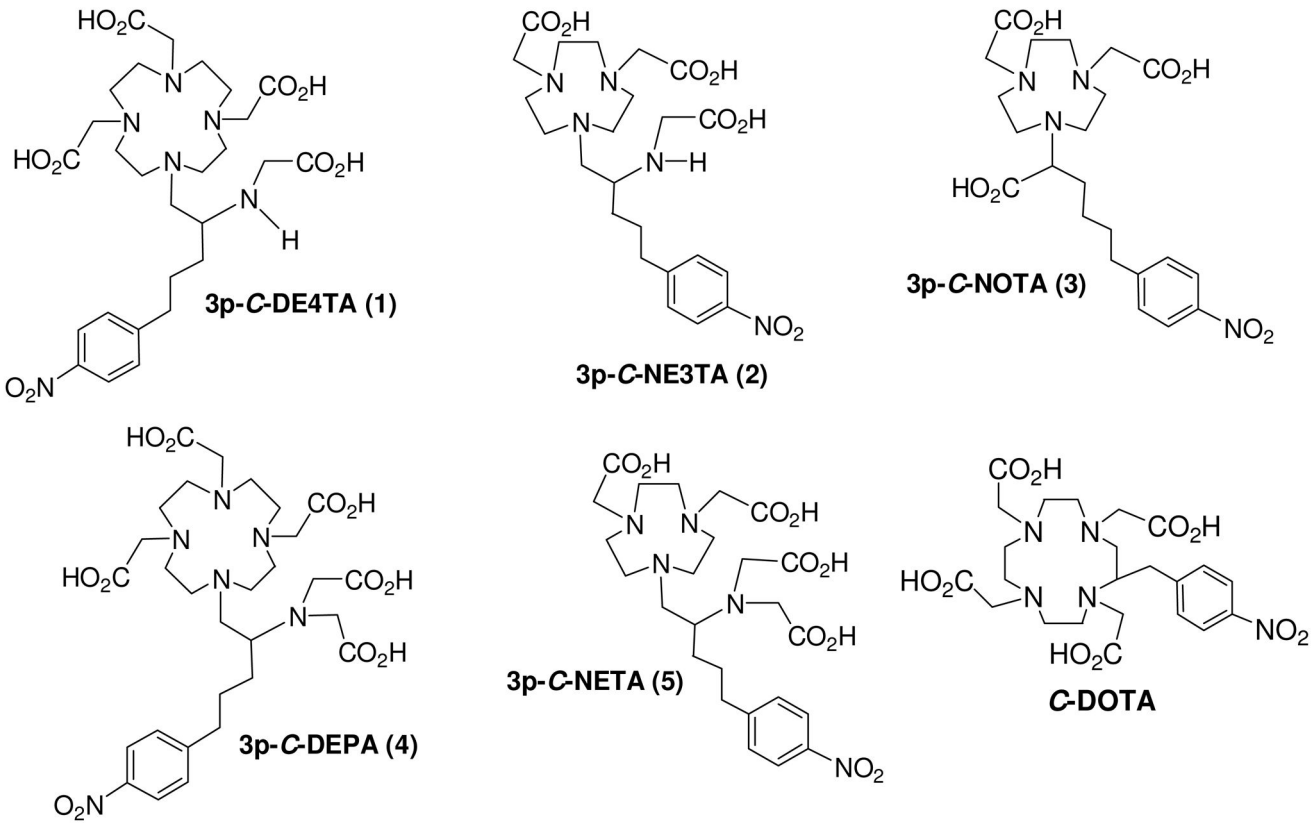

Figure 1.
Bifunctional Chelators for targeted radioimmunotherapy using ^{90}Y and ^{177}Lu in preclinical evaluation

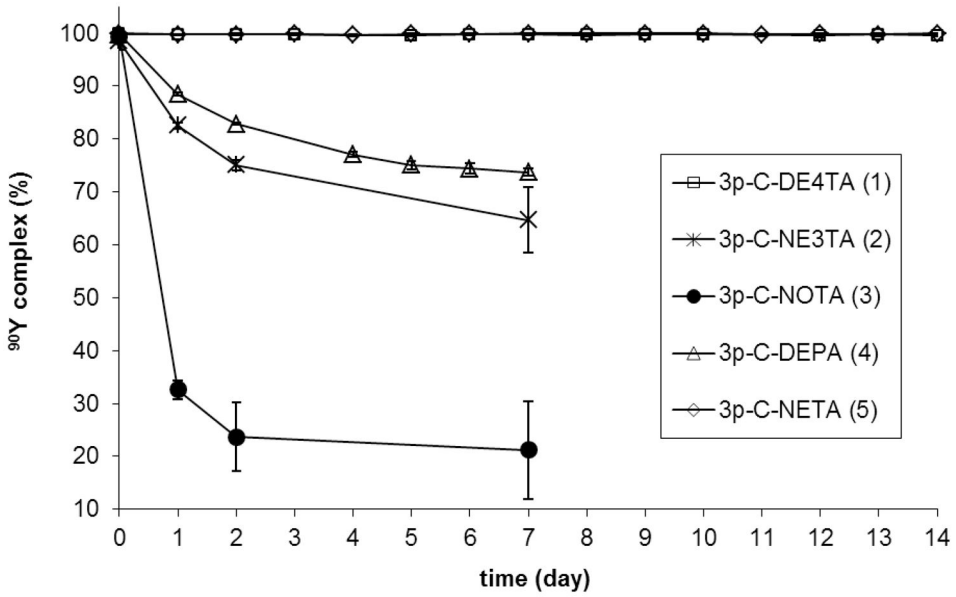

Figure 2.
In vitro serum stability of ^{90}Y-radiolabeled complexes (pH 7 and 37 °C)

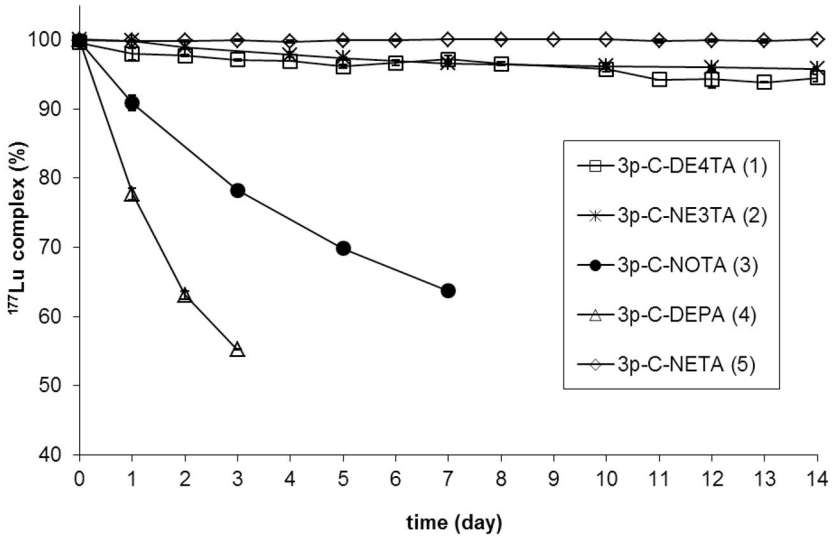

Figure 3.
In vitro serum stability of ^{177}Lu-radiolabeled complexes (pH 7 and 37 °C)

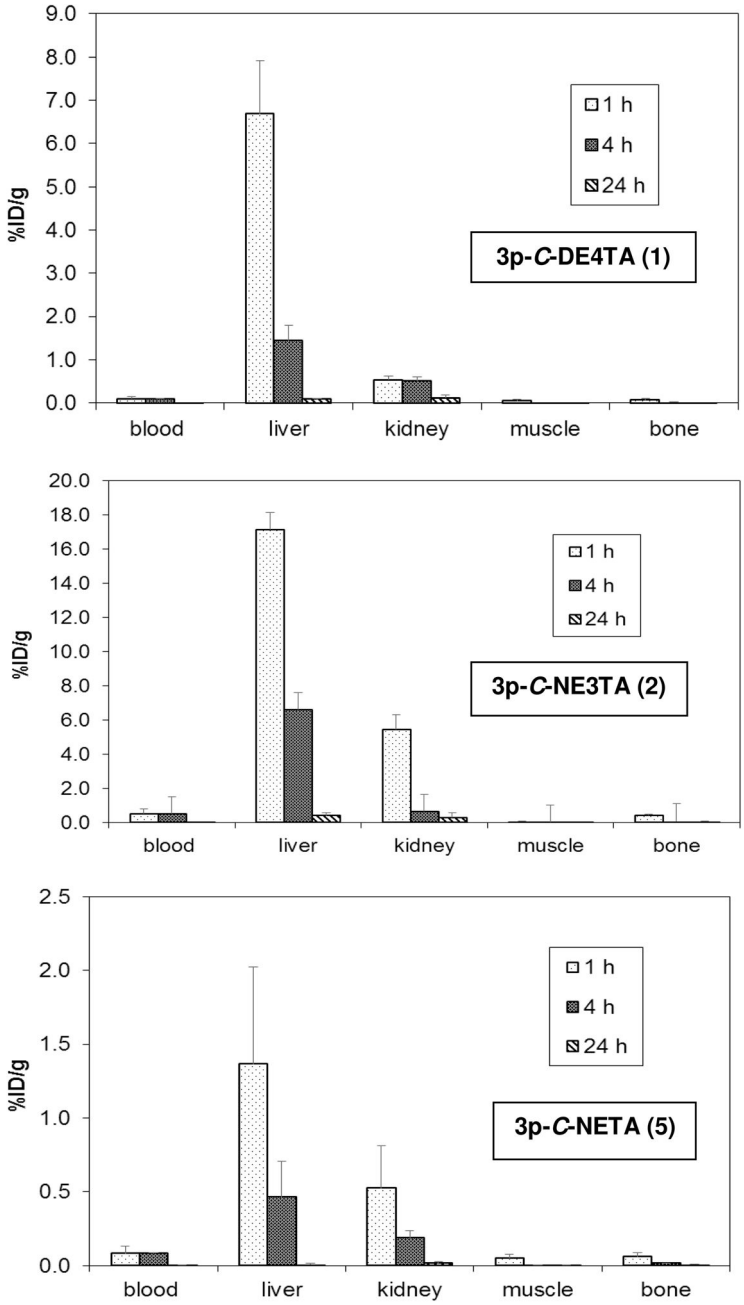

Figure 4.
Biodistribution of ^{177}Lu-radiolabeled chelates in Non-Tumor Bearing CF-1 Mice.

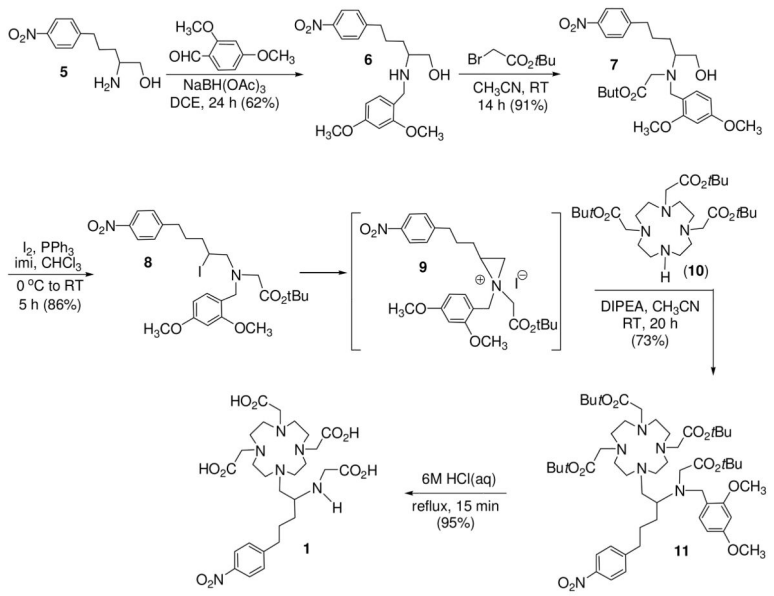

Scheme 1.
Synthesis of 3p-*C*-DE4TA (1)

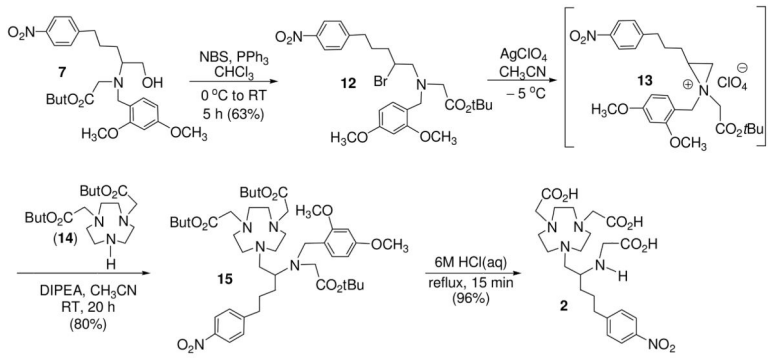

Scheme 2.
Synthesis of 3p-*C*-NE3TA (2)

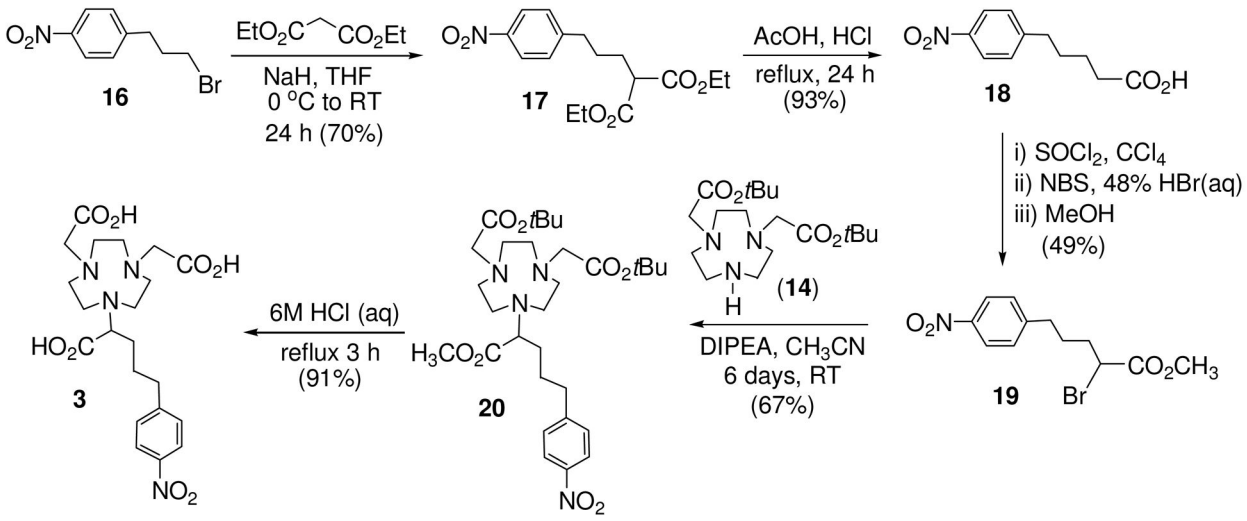

Scheme 3.
Synthesis of 3p-*C*-NOTA (3)

Table 1

Radiolabeling efficiency (%) of bifunctional chelates with ^{90}Y (pH 5.5, RT)[#]

Time (min)	Radiolabeling efficiency (%)					
	3p-*C*-DE4TA[*] (1)	3p-*C*-NE3TA[‡] (2)	3p-*C*-NOTA[‡] (3)	3p-*C*-DEPA (4)	3p-*C*-NETA[+] (5)	*C*-DOTA[+]
1	88.4 ± 1.9	3.1 ± 0.28	10.3 ± 0.6	89.3 ± 2.8	97.4 ± 0.7	77.1 ± 3.7
10	99.2 ± 0.58	22.5 ± 0.28	50.8 ± 1.8	96.8 ± 0.5	98.7 ± 1.6	69.4 ± 10.6
20	99.3 ± 0.61	37.6 ± 0.64	73.9 ± 0.6	98.0 ± 0.9	98.7 ± 2.2	71.2 ± 11.2
30	99.2 ± 0.72	49.1 ± 1.6	82.7 ± 0.4	97.9 ± 0.2	99.4 ± 0.9	76.1 ± 9.52
60	99.5 ± 0.49	68.7 ± 3.4	89.3 ± 0.1	98.5 ± 0.2	99.5 ± 1.0	83.5 ± 8.13

[#]Radiolabeling efficiency (mean ± standard deviation%) was measured in triplicate using ITLC.

[*]Radiolabeling efficiency was determined at pH 7 using ITLC.

[‡]Duplicate run

[+]The data were cited for comparison.[16]

Table 2

Radiolabeling efficiency (%) of bifunctional chelates with ^{177}Lu (pH 5.5, RT)[#]

Time (min)	Radiolabeling efficiency (%)					
	3p-*C*-DE4TA[*] (1)	3p-*C*-NE3TA (2)	3p-*C*-NOTA (3)	3p-*C*-DEPA (4)	3p-*C*-NETA[+] (5)	*C*-DOTA[+]
1	85.2 ± 0.7	6.7 ± 0.1	17.5 ± 0.5	93.9 ± 1.3	100.0 ± 0.0	94.5 ± 3.9
10	99.8 ± 0.3	36.6 ± 0.4	81.3 ± 0.2	98.7 ± 0.2	100.0 ± 0.0	99.5 ± 0.5
20	99.8 ± 0.1	63.2 ± 0.8	95.0 ± 0.2	99.2 ± 0.3	100.0 ± 0.0	99.9 ± 0.1
30	99.9 ± 0.1	78.1 ± 1.1	99.1 ± 0.4	99.4 ± 0.1	100.0 ± 0.0	99.9 ± 0.1
60	100.0 ± 0.1	95.0 ± 0.1	100 ± 0.1	99.3 ± 0.2	100.0 ± 0.0	100.0 ± 0.0

[#]Radiolabeling efficiency (mean ± standard deviation%) was measured in triplicate using ITLC.

[*]Radiolabeling efficiency was determined at pH 7 using ITLC.

[+]The data cited for comparison.[16]

Bioorg Med Chem. Author manuscript; available in PMC 2016 March 01.